

Simulation of Near Fault Ground Motion of the Earthquake of November 1759 with magnitude of 7.4 along Serghaya Fault, Damascus City, Syria

Hussam Eldein Zaineh, Hiroaki Yamanaka & Yadab Prasad Dhakal
Department of Environmental Science and Technology, Tokyo Institute of Technology, Japan

Rawaa Dakkak
National Earthquake Center (NEC), Syria

Mohamad Daoud
Higher Institute of Earthquake Studies and Research, Syria



SUMMARY:

The seismic hazard potential for Damascus city is mainly controlled by the Serghaya Fault which is a branch of the Dead Sea Fault System (DSFS). Ground motion in Damascus city was estimated for the November 1759 earthquake along the fault. The Kostrov-like slip-velocity function was used as an input to the Discrete Wave Number Method to simulate the near-fault ground motions of the Earthquake of November 1759 for broadband frequencies (0.1 – 6 Hz). In order to model the incoherent rupture time which excites large high-frequency waves, the difference between the actual rupture time and the coherent (average) rupture time is introduced (Δt_r). The simulated high frequency (1.0 – 6.0 Hz) near fault ground motions are much higher than the design requirements defined by the Syrian building code 2004. That reflects the importance of increasing the design earthquake loads in the case of near-fault ground motions. The results of the 1-D site response analysis show that the high frequency ground motions are significantly exaggerated by the effect of the shallow structure in the case of the eastern part of Damascus city as well as the central part along Barada River. The synthetic broadband ground motions are compared in terms of MMI intensity calculated from the modified PGV values of the synthetic waveforms with the observed intensity values. The calculated intensities are in good agreement with the observed one at most sites that validate the proposed source model of Nov. 1759 earthquake.

Keywords: Strong ground motion simulation, Kostrov slip-velocity function, Seismic hazard of Damascus city

1. INTRODUCTION

Many recent earthquakes took a heavy toll of lives and caused great property damages in the cities near the focal region (e.g. Northridge earthquake 1994 and 1995 Hyogo-ken Nanbu earthquake). It is very important for the earthquake resistant design of structures to understand the basic characteristics of near-field ground motions. Investigating the earthquake loads by considering the near-field ground motions is an important issue for earthquake damage mitigation. Damascus city located about 30 km south east of Serghaya fault, might suffer a great damage in the case of big earthquake. Serghaya fault, as a branch of Dead Sea Fault System (DSFS), is considered as the main source of seismic risk potential for the city, and through the last 2000 years, many destructive earthquakes occurred in the region and caused much causality in Damascus city and its vicinity. Historical seismicity suggests that DSFS is capable of generating large earthquakes which mean a significant seismic hazard in this region (N. N. Ambraseys, 2009). One of the most destructive historical events occurred in November 25, 1759. This earthquake has been well documented and the macroseismic data suggest a magnitude of about 7.4 and up to 100 km of surface rupture probably along the Yammouneh fault in the Bekaa valley and caused heavy damage with great loss of life in numerous villages and towns, including Damascus, Beirut and Baalbek.

In Damascus city, the shock caused great panic, several casualties, and considerable, but reparable, damage. Destruction was heavier in the upper reaches of the Barada River at Serghaya and Hasbaya while, Baalebek was totally destroyed with great loss of life (Ambraseys & Barazangi 1989). Figure 1 shows the intensity distribution of the main shock of November 25, 1759 while, Table 1 shows the

largest historical earthquakes in western Syria and Lebanon (32.5° – 35.5° N).

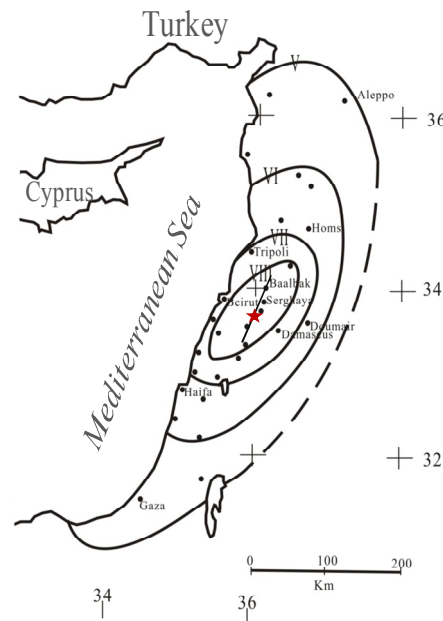


Figure 01, Intensity distribution of the main shock of November 25, 1759; intensities in the MSK scale (Ambraseys & Barazangi 1989)

Table 01, large historical earthquakes in western Syria and Lebanon (32.5° – 35.5° N)

Year	M	Affected areas (in order of decreasing intensity)
198 BC	?	Lebanese Coast, Southern Syria
115 AD	?	Northwest Syria
303 AD	~7.0	Lebanese coast, Southern Syria
551 AD	7.0-7.5	Lebanese coast
749 AD	7.0-7.5	Southern Bekaa Valley, Southern Syria
859 AD	7.0-7.5	Northwest Syria
991 AD	7.0-7.5	Bekaa Valley, Anti Lebanon
1063 AD	~7.0	Northern Lebanese coast, Syrian Coast
1157 AD	7.0-7.5	Northwest Syria, Ghab Valley
1170 AD	>7.5	Northern Lebanon, Syrian Coast
1202 AD	>7.5	Mt. Lebanon, Bekaa Valley, Hula Basin, Lebanese-Syrian Coast
1705 AD	~7.0	Anti-Lebanon, Zabadani and Bekaa V., Damascus, Northern Lebanese Coast
1759 AD	~7.4	Bekaa V., Anti-Lebanon, Golan Heights, Mt. Lebanon, Damascus
1837 AD	7.0-7.5	Western Lebanon, Southern Bekaa V., Hula Basin

Data from Poirier & Taher (1980), Ambraseys & Barazangi (1989), Ambraseys & White (1997), Ambraseys & Jackson (1998) and Sbeinati et al. (2003)

2. TECTONIC SETTINGS

The Dead Sea Fault System (DSFS) forms the plate boundary that links the Arabian plate convergence in southern Turkey with the active seafloor spreading in the Red Sea. This system evolved since mid-Cenozoic time as a result of the breakup of the Arabian plate from the African plate. The present-day relative motion between Arabian plate and African plate is estimated to be 4-8 mm yr⁻¹, based on plate models (e.g. Joffe & Garfunkel 1987; Jestin et al. 1994) and recent GPS observations (e.g. McClusky et al. 2000, 2003). This is consistent with geological estimates of Quaternary slip rates for the southern DSFS (e.g. Garfunkel et al. 1981; Klinger et al. 2000a). Branching from southern part of DSFS in the Golan Heights, Serghaya fault can be traced approximately 125 km through the Anti

Lebanon Mountains to the eastern edge of the Bekaa Valley (located approximately along the Syrian-Lebanese border). Shear indicators demonstrate predominately left-lateral slip. Rakes of 10 – 20 are observed on sub-vertical fault planes, implying a ratio of strike-slip to dip-slip between 4:1 and 5:1; the strike of Serghaya fault is taken to be N20°E, and the dip is about 70° (Gomez et. al. 2003). The recent studies of Serghaya fault revealed that Serghaya fault is an active fault. The total fault length and 2.0-2.5m displacements with historical seismicity, suggest that the fault may be capable of generating large ($M \sim 7$) earthquakes (e.g. Gomez et. al. 2003). These studies provide an evidence for a surface-rupturing event within the 18th century along Serghaya fault. This event involved 2-2.5 m of mainly left-lateral dislocation and may correspond to one of two historically documented earthquakes during the 18th century (in 1705 and 1759) (e.g. Gomez et. al. 2001, 2003).

In this study, we simulate the broad band near-fault ground motions of the earthquake of November 25, 1759 (The earthquake is assumed to be generated by Serghaya fault) for different sites; Namely, MRJ, HOS & TOT sites situated in Damascus city where the observed intensity at these sites varied from VII to VIII as well as one sites located in the Eastern Damascus Suburb (DMR), this site located about 60 km to the east of the epicentre and the observed intensity is slightly less than VII.

3. GROUND MOTION SIMULATION

3.1. Green's function

The response of horizontally layered crustal structures, due to a double-couple point source or Green's function, has been calculated by the discrete wave number method (Bouchon et al. 1977; Bouchon 1979, 1981) for a particular focal mechanism and source time function. To simulate the near field ground motion, it is essential to model how the rupture initiates, spreads, and stops on the fault and how dynamic slip velocity is developed under shearing stress. The Kostrov-like slip-velocity source time functions, which represent the stress conditions on and around the fault, were used widely to simulate the high frequency near field ground motions (eg. Archuleta and Hartzell, 1981...). In this study, we follow the kinematic source model introduced by Nakamura & Miyatake (2000) as a slip-velocity source time functions.

3.2. Source Modelling

As an assumption frequently made in seismology is that a large earthquake can be simulated by a grid of point dislocations (e.g., Archuleta and Hartzell, 1981). The fault plane and the asperities were subdivided into several sub-faults and each sub-fault is treated as a point source. The ground motions at an observation site produced by the rupture of individual sub-faults are summed with time lags to account for rupture propagation on the fault plane. Since the actual rupture velocity probably fluctuates significantly in realistic situations (Das and Aki, 1977; Mikumo and Miyatake, 1978; Archuleta, 1982) and this fluctuation excites strong high-frequency waves (e.g., Madariaga, 1977); we introduce the effects of the variable rupture velocities in the summation process by dividing the rupture time t_r into the coherent (average) rupture time and the incoherent rupture time Δt_r as follows:

$$t_r = \frac{x}{V_r} + \Delta t_r$$

$$\begin{aligned} \text{for } \frac{x}{V_r} > 2.0\text{sec}, & \quad -0.5s \leq \Delta t_r \leq 0.5s \\ \text{for } \frac{x}{V_r} \leq 2.0\text{sec}, & \quad -0.1 \frac{x}{V_r} \leq \Delta t_r \leq 0.1 \frac{x}{V_r} \end{aligned} \quad (3.1)$$

Where, V_r is the average rupture velocity, x is the distance from the rupture front to the starting rupture point. Therefore, to include the effects of fluctuations at the rupture front we introduce Δt_r as the difference between the smooth rupture time and the coherent one. We introduce Δt_r as random numbers that are uniform in the above mentioned ranges.

We simulate the earthquake of 1759 with moment magnitude of ~ 7.4 . The total fault rupture length (L) is assumed to be about 100 km along Serghaya fault and the total width (W) is about 20 km. We assumed two asperities in the entire fault rupture; the combined area of asperities (S_a) is specified to be about 22% of fault's area (Somerville et al. 1999; Irikura and Miyake 2001). The other source parameters were estimated by following the empirical relationships proposed by Irikura (2004), and they are summarized in Table 02. The seismogram from each point source is obtained numerically by the Discrete Wave Number Method of Bouchon (1979, 1981). The point sources within asperities and background region have the following focal mechanism: Strike $N20^\circ E$, dip 70° and rake 15° . Figure 02a shows Damascus city with the assumed fault line. Figure 02b, shows the proposed fault model with the asperities; stars show the rupture starting points. We used the smoothed ramp function as a source time function for the background region while for asperities we used Kostrov slip-velocity function as a source time function. The approximation formula by Nakamura and Miyatake (2000) is used for this slip-velocity time function for the asperity case.

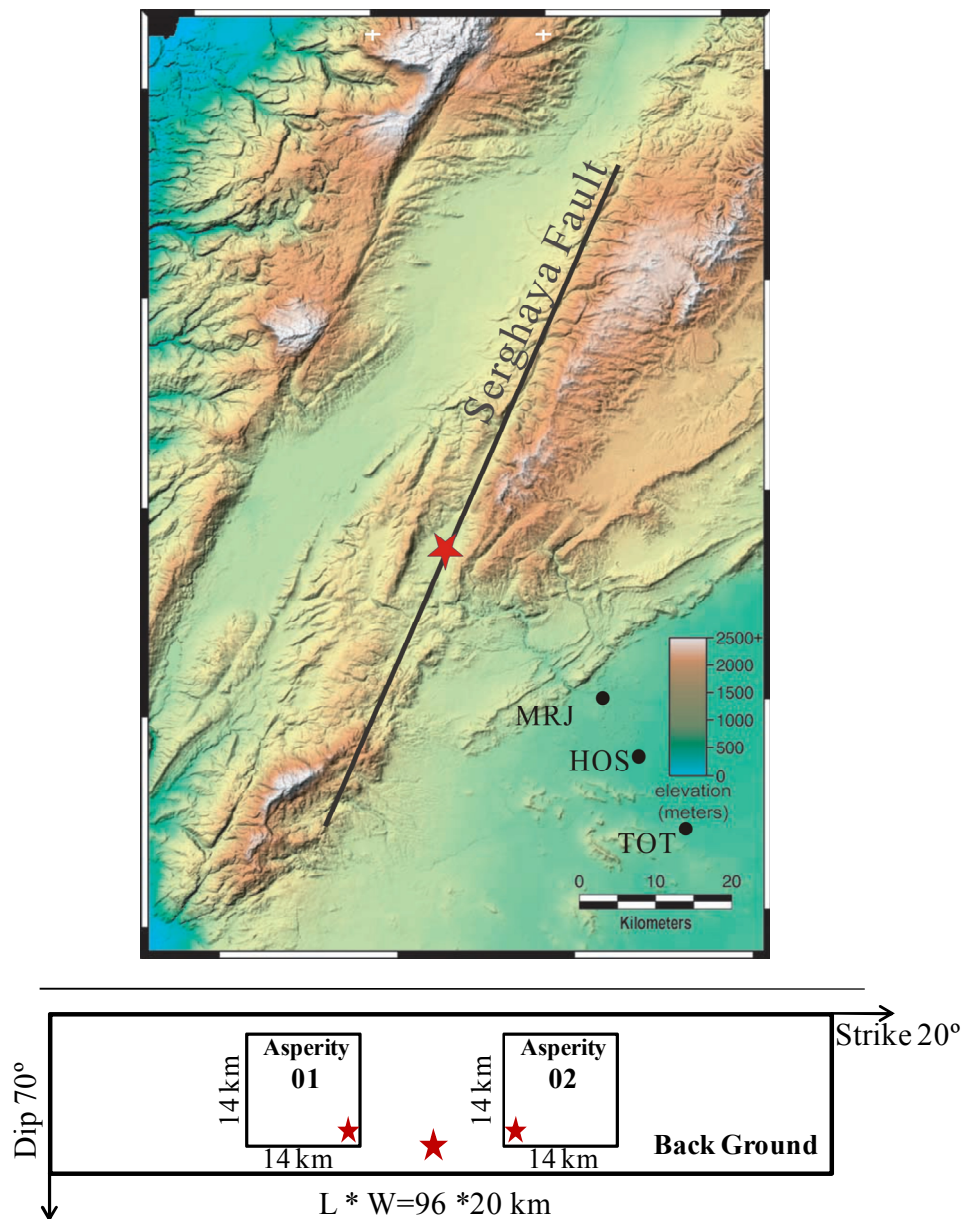


Figure 2, (a) Location of MRJ, HOS & TOT sites (in Damascus city) with the assumed fault line, star shows the epicentre location. **(b)** The proposed fault model with the asperities, stars show the rupture starting points.

Table 02, Assumed source parameters of the November 1759 Earthquake

	<i>Area</i> (<i>L*W</i>)km	<i>M_o</i> (<i>N.m</i>)	<i>f_{max}</i> (<i>Hz</i>)	<i>τ_r</i> (<i>s</i>)	<i>V_r</i> (<i>Km/s</i>)	<i>σ</i> (<i>bar</i>)
<i>Asperity 1</i>	<i>14*14</i>	<i>2E+19</i>	<i>6.0</i>	<i>1.6</i>	<i>2.25</i>	<i>90</i>
<i>Asperity 2</i>	<i>14*14</i>	<i>2E+19</i>	<i>6.0</i>	<i>1.6</i>	<i>2.25</i>	<i>90</i>
<i>background</i>	<i>96*20</i>	<i>6E+19</i>	<i>6.0</i>	<i>1.8</i>	<i>2.25</i>	<i>40</i>

τ_r =rise time; V_r = rupture velocity; σ = stress drop

4. VELOCITY STRUCTURE

We use a flat-layered velocity structure obtained by overlapping the crustal velocity model under Syria (Ibrahim et al. 2007) with the uniform shallow velocity structure under Damascus basin (Zaineh et al. 2012). Ibrahim et al. (2007) estimated the 1-D velocity model of the crust and uppermost mantle under Syria from the local earthquake data recorded by the Syrian National Seismological Network during 1995-2004. While the shallow S-wave velocity structure in Damascus city was estimated by using microtremor exploration (Zaineh et al. 2012). In our simulation, we considered the layer with S-wave velocity of ~1600 m/s as a uniform shallow layer overlain the crustal model; the thickness of this layer was assumed to be uniform beneath Damascus basin (~0.4 km). While, the effect of the uppermost shallow layers (including the engineering bedrock) on seismic ground motions will be estimated independently for each site following a 1_D site response analysis. Table 03 shows the combined 1-D velocity model used in simulation; the first layer (***bold italic***) represents the uniform shallow velocity structure under Damascus city while the other layers represent the deep velocity model beneath Syria.

Table 03, the combined 1-D velocity model used for simulation.

V_p (km/s)	V_s (km/s)	H(km)	ρ (t/m ³)	Q_p	Q_s
<i>3.00</i>	<i>1.60</i>	<i>0.60</i>	<i>2.20</i>	<i>100</i>	<i>40</i>
5.68	2.99	4.00	2.50	500	200
5.87	3.48	6.00	2.60	500	200
6.18	3.48	8.00	2.70	500	200
6.74	3.95	20.00	2.80	500	200
8.00	3.64	----	3.10	500	200

V_p & V_s =P-wave and S-wave velocities; H=layer thickness; ρ =mass density; Q_p & Q_s =quality factor of P-wave and S-wave respectively

5. SIMULATION RESULTS

We simulate the ground motions of the earthquake of November 1759 at the sites of MRJ, HOS and TOT located in Damascus city which experience a considerable but reparable damage; as well as one site (DMR) located in the Eastern Damascus Suburb. The site of DMR is about 30 km to the north east of Damascus city and the damage in this town was less significant than the damage in Damascus city.

Figures 3 and 4 present the velocity and acceleration time histories simulated at the all sites for the proposed source model. All the waveforms were normalized for plotting and the maximum peak values are presented on the figures. Large values of peak ground velocity (PGV) and peak ground acceleration (PGA) were obtained at MRJ site located in the centre of the city which is the nearest site to the epicentre (51.3 cm/s and 896.4 gal). The values of PGV and PGA attenuated gently at the other sites with distance from the epicentre.

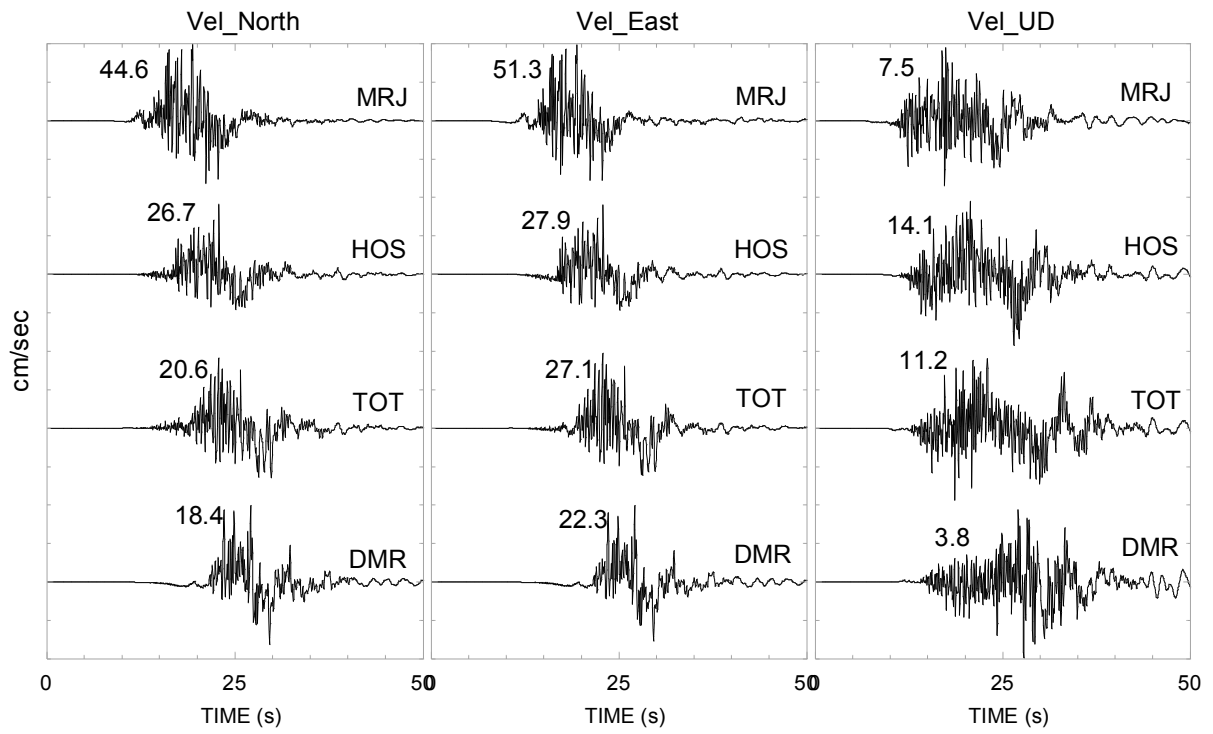


Figure 03, Simulated velocity waveforms at the all sites.

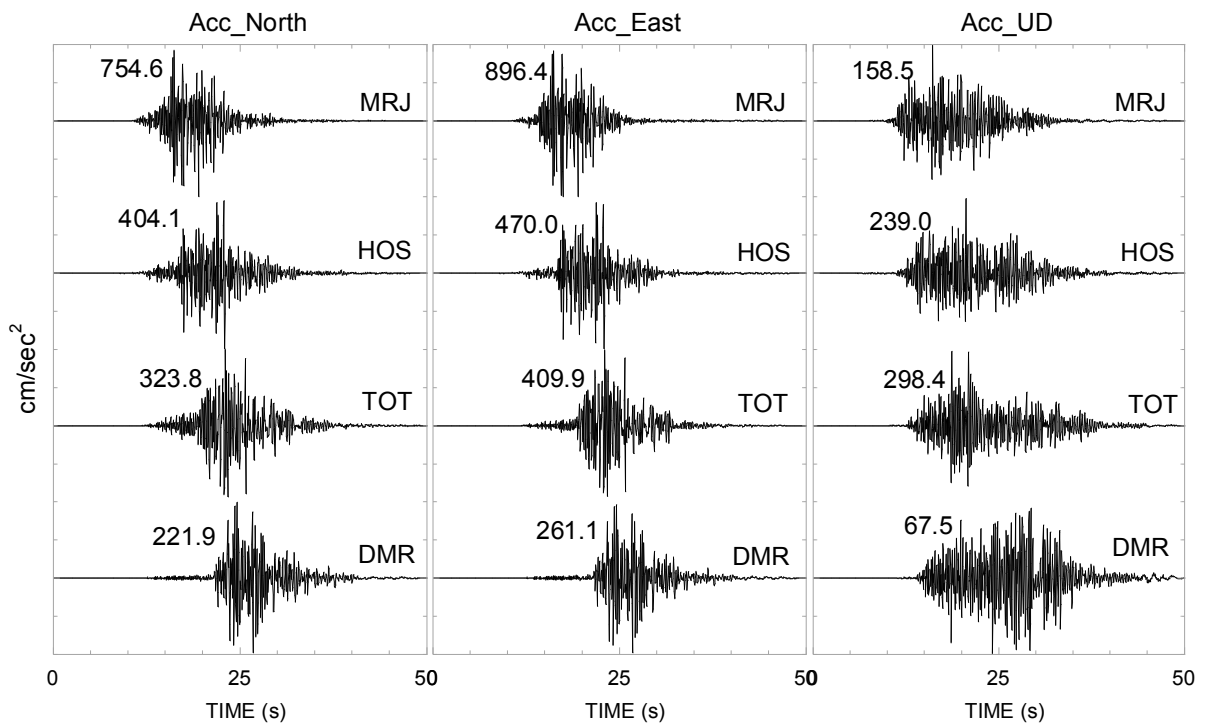


Figure 04, Simulated acceleration waveforms for the all sites.

6. DISCUSSION AND CONCLUSIONS

We simulate the near-fault ground motions of the November 1759 Earthquake for broadband frequencies (0.1 – 6 Hz). In our simulation, we used the Kostrov-like slip-velocity function as an input to the discrete wave number method. In order to model variable rupture velocities, we introduce the incoherent rupture time Δt_r as the difference between the actual rupture time and the coherent one.

For earthquake damage reduction, the earthquake resistant design of structures should consider the characteristics of the near-fault ground motions. Figure 5 shows the acceleration response spectra for the all sites for a 5% of damping; the thick gray line represents the acceleration design response spectrum defined by the Syrian building code (2004) for stiff sites (soil type B). For the high frequency range (1.0 – 6.0 Hz), the simulated ground motions look much higher than the design requirements defined by the Syrian building code. That reflects the importance of increasing the design earthquake loads in the case of near-fault ground motions (especially for the high frequency range).

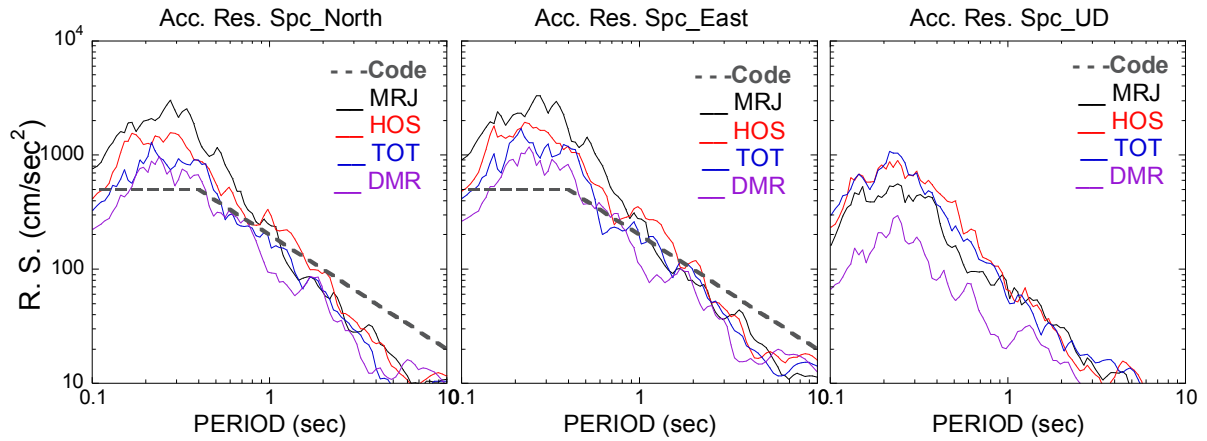


Figure 05, Comparisons of the acceleration response spectra (5% damping) for the all sites; the gray dashed line represents the acceleration design response spectrum for the stiff sites (Syrian building code 2004)

It was revealed that the shallow structure which is not uniform in Damascus city has a major contribution to the high frequency amplification; the sites in the eastern part of Damascus as well as the central part along Barada River have the highest amplification (Zaineh et al. 2012). Figure 6 shows an example of the 1-D site response analysis for MRJ and TOT sites that belong to different categories in Damascus city. It is clear that the high frequency ground motions are significantly exaggerated by the effect of the shallow structure in the case of the eastern part of the city as well as the central part along Barada River (MRJ site in Figure 6).

Furthermore, it is important to note that the dominant periods of the most residential buildings in Damascus city are within the high frequency range (1.0 – 6.0 Hz); the simulated ground motions look much higher than the design requirements defined by the Syrian building code in this frequency range as well. This indicates the importance of simulating the high frequency ground motion as well as considering the high frequency amplification which associated with the shallow structure in Damascus city.

To perform a validation of the proposed source model and the results of the simulated waveforms, the PGV values of the synthetic waveforms were multiplied by the average of amplification factor to consider the effect of the shallow structure. Then we calculated MMI intensity using the modified values of PGV and compared the obtained intensities with the observed MSK intensities of the November 1759 earthquake (Ambraseys & Barazangi, 1989). We follow the empirical equation (6.1) introduced by Wald et al. (1999). The calculated Intensities and the observed one are shown in Table

04. It looks that the calculated intensities are in good agreement with the observed one at the most sites that validate our proposed source model of Nov. 1759 earthquake.

$$I_{mm} = 3.47 \log(PGV) + 2.35 \quad (6.1)$$

Table 04, Calculated and observed Intensities

station	Ave. Site Ampl.	PGV_H	I_{CAL}	I_{OBS}
MRJ	2.16	103.3	9.3	VII-VIII
HOS	1.87	51.0	8.3	VII-VIII
TOT	1.50	35.4	7.7	VII-VIII
DMR	1.50	30.4	7.5	VI-VII

PGV_H = modified horizontal peak ground velocity; I_{CAL} and I_{OBS} = the calculated and the observed intensities

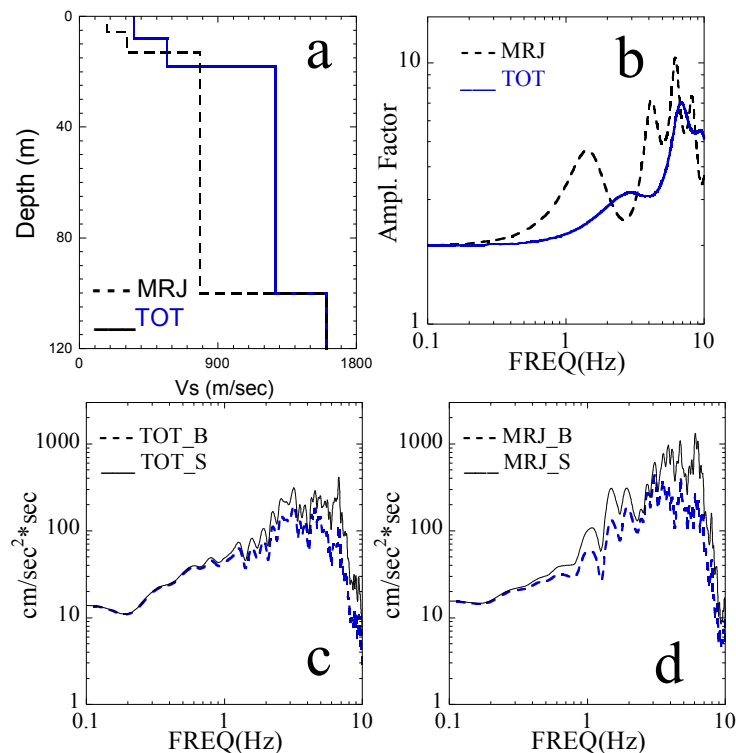


Figure 6, (a) 1-D shallow structure at MRJ and TOT sites in Damascus city; (b) calculated site amplification at both sites; (c) and (d) acceleration fourier spectra of the simulated ground motion at the basement (dashed line) and the surface (solid line) for TOT and MRJ sites respectively.

ACKNOWLEDGEMENTS

We acknowledge the financial support of Center for Urban Earthquake Engineering (CUEE) under the G-COE program of Tokyo Institute of Technology.

REFERENCES

- Ambraseys N.N., (2009) Earthquakes in the Mediterranean and Middle East –A Multidisciplinary Study of Seismicity up to 1900, 583–586.
- Ambraseys N.N., and M. Barazangi, (1989) The 1759 earthquake in the Bekaa Valley: implications for earthquake hazard assessment in the Eastern Mediterranean region, *J. geophys. Res.*, **94**, 4007–4013
- Ambraseys N.N., and Jackson J.A., (1998) Faulting associated with historical and recent earthquakes in the Eastern Mediterranean region. *Geophys. J.Int.*, **133**, 390–406.
- Ambraseys N.N., and White D., (1997) The seismicity of the eastern Mediterranean region 550–1 BC: a re-appraisal. *J. Earthquake Eng.*, **1**, 603–632.

- Archuleta, R. and S. Hartzell (1981) Effects of fault finiteness on near source ground motion, *Bull. Seism. Soc. Am.* **71**, 939-957
- Archuleta, R. J. (1982) Analysis of near source station and dynamic measurements from the 1979 Imperial Valley earthquake, *Bull. Seism. Soc. Am.* **72**, 1927-1956
- Bouchon M., (1979) Discrete wave-number representation of Elastic Wave Fields in Three-space Dimensions. *J. Geophys. Res.*, **84**, 3609-3614
- Bouchon M., and Aki K., (1977) Discrete Wave-Number Representation of Seismic Source Wave Fields. *Bull. Seism. Soc. Am.* **67-2**, 259-277
- Bouchon M., (1981) A Simple Method to Calculate Green's Functions for Elastic Layered Media, *Bull. Seism. Soc. Am.* , **71**, 959-971.
- Das, S., and K. Aki (1977) Fault plane with barriers: a versatile earthquake model, *Geophys. J. R. Astr. Soc.* **50**, 643-668
- Garfunkel Z., Zak I. and Freund, R., (1981) Active faulting in the Dead Sea rift, *Tectonophysics*, **80**, 1-26
- Gomez F. et al., (2001) Coseismic displacements along the Serghaya fault: an active branch of the Dead Sea fault system in Syria and Lebanon, *J. geol. Soc. Lond.*, **158**, 405-408
- Gomez F. et al., (2003) Holocene faulting and earthquake recurrence along the Serghaya branch of the Dead Sea fault system in Syria and Lebanon, *Geophys. J. Int.*, **153**, 658-674
- Irikura K., and Miyake H., (2001) Prediction of strong ground motions for scenario earthquakes. *Journal of Geography* **110**, 849-875 (in Japanese with English abstract)
- Irikura K., et al., (2004) Recipe for Predicting Strong Ground Motion from Future Large Earthquake. *Proceedings of the 13th World Conference on Earthquake Engineering* No. 1371
- Ibrahim R., (2007) 1-D Velocity model for Syria from local earthquake data. Master Thesis, GRIPS University, Japan
- Jestin F., Huchon P. and Gaulier J.M., (1994) The Somalia plate and the Eastern Africa Rift System: present-day kinematics. *Geophys. J. Int.*, **116**, 637-654
- Joffe S. and Garfunkel Z., (1987) Plate kinematics of the circum Red Sea—a re-evaluation, *Tectonophysics*, **141**, 5-22
- Klinger, Y. et al., (2000a) Slip rate on the Dead Sea transform fault in the northern Araba Valley (Jordan), *Geophys. J. Int.*, **142**, 755-768.
- Kostrov B. V., (1964) Self-similar problems of propagation of shear cracks, *J. Appl. Math. Mech.* **28**, 1077-1087.
- McClusky S. et al., (2000) GPS constraints on plate motion and deformation in the eastern Mediterranean: Implications for plate dynamics, *J. geophys. Res.*, **105**, 5695-5719
- McClusky S. et al., (2003) GPS Constraints on Africa (Nubia) and Arabia plate motions, *Geophys. J. Int.*, **155**, 126-138
- Miyatake T., and Nakamura H., (1998) "An approximate solution for slip rate and slip acceleration time function in dynamic rupture propagation with slip weakening friction", the third symposium on the natural disaster by near-field great earthquake, 67-68
- Madariaga R., (1976) Dynamics of an expanding circular fault, *Bull. Seism. Soc. Am.* **66**, 639-666
- Madariaga, R. (1977) High frequency radiation from crack (stress drop) models of earthquake faulting, *Geophys. J. R. Astr. Soc.* **51**, 625-651
- Mikumo, T., and T. Miyatake (1978) Dynamic rupture process on a three-dimensional fault with non-uniform frictions and near-field seismic waves, *Geophys. J. R. Astr. Soc.* **54**, 417-438
- Poirier J.P., and Taher M.A., (1980) Historical seismicity in the Near and Middle East, North Africa, and Spain from Arabic documents (VIIth-XVIIIth century). *Bull. Seism. Soc. Am.*, **70**, 2185-2201
- Somerville P., et al., (1999) Characterizing earthquake slip models for the prediction of strong ground motion. *Seismol Res Lett* **70**, 59-80
- Sbeinati M.R., Darawcheh R., and Mouty M., (2005) The historical earthquakes of Syria: an analysis of large and moderate earthquakes from 1365 B.C. to 1900 A.D., *Ann. Geofis.*, 48-3
- Wald, D. J., V. Quitoriano, T. H. Heaton, and H. Kanamori (1999) Relationships between peak ground acceleration, peak ground velocity, and 1874 G.-A. Tselentis and L. Danciu modified Mercalli intensity in California, *Earthq. Spectra* **15-3**, 3 557-564
- Zaineh H. E., et al. (2012) Estimation of Shallow S-Wave Velocity Structure in Damascus City Syria, Using Microtremor Exploration, *J. of Soil Dyn. and Earthq. Eng.* **39**, 88-99